The Effect of Al_2O_3 Barrier Layers in TiO_2/Dye/CuSCN Photovoltaic Cells Explored by Recombination and DOS Characterization Using Transient Photovoltage Measurements

B. C. O'Regan,* S. Scully, and A. C. Mayer

Energy Research Center Netherlands, P.O. Box 1 1755 ZG Petten, The Netherlands

E. Palomares and J. Durrant

Department of Chemistry, Imperial College London, London SW7 2AZ

Received: July 19, 2004; In Final Form: December 19, 2004

Solid-state dye-sensitized solar cells of the type TiO_2/dye/CuSCN have been made with thin Al_2O_3 barriers between the TiO_2 and the dye. The Al_2O_3-treated cells show improved voltages and fill factors but lower short-circuit currents. Transient photovoltage and photocurrent measurements have been used to find the pseudo-first-order recombination rate constant (k_{pfo}) and capacitance as a function of potential. Results show that k_{pfo} is dependent on V_{oc} with the same form as in TiO_2/dye/electrolyte cells. The added Al_2O_3 layer acts as a "tunnel barrier", reducing the k_{pfo} and thus increasing V_{oc}. The decrease in k_{pfo} also results in an increased fill factor. Capacitance vs voltage plots show the same curvature (∼150 mV/decade) as found in TiO_2/dye/electrolyte cells. The application of one Al_2O_3 layer does not cause a significant shift in the shape or position of the capacitance curve, indicating that changes in band offset play a lesser role in the observed V_{oc} increase. Cells made with P25 TiO_2 have, on average, 2.5 times slower recombination rate constants (longer lifetimes) than those made with colloidal TiO_2. The cells with P25 also show 2.3 times higher trap density (DOS), which results in little change in the V_{oc} between the two types of TiO_2. It is further noted that the recombination current in these cells cannot be calculated from the total charge times the first order rate constant.

Introduction

Dye-sensitized liquid-junction solar cells have been under active development for the past decade.[1−13] More recently, solid-state dye-sensitized cells have been developed where the liquid electrolyte is replaced by a molecular hole conductor or p-type semiconductor.[14−18] Dye-sensitized cells with an n-type oxide and p-type hole conductor have also been referred to as dye-sensitized heterojunctions (DSHs) by virtue of the placement of the light-absorbing dye at an otherwise transparent n−p heterojunction.[19,20] The promise of DSHs in the realm of photovoltaics is the fusion of the inexpensive materials of the dye-sensitized liquid-junction technology with the easier and less expensive manufacturing and packaging applicable to solid devices.

In dye-sensitized cells, light absorption occurs in a monolayer of dye at the interface between a transparent oxide electron conductor (usually TiO_2) and a transparent electrolyte. Sufficient light absorption is achieved by using a thick layer (∼10 μm) of nanosized oxide particles (∼20 nm) wherein all the internal surface is coated with the dye. In the liquid electrolyte cells, the pores are completely filled with the electrolyte. In the solid-state version of this cell, the pores are filled with a solid, transparent hole conductor. This nanocomposite has a structure that has been referred to as an "interpenetrating network heterojunction", or a "bulk heterojunction". We will use "interpenetrating heterojunction", or the abbreviation "i-het", for the physical structure and DSH for the device concept.

One of the proposed materials for the p-type side of a DSH is CuSCN.[19,21−24] The fabrication and functioning of the dye-sensitized cells with CuSCN has been presented in the literature,[25,26] and only relevant parts will be described in detail. Inside the interpenetrating p−n heterojunction, only the dye layer absorbs visible light. After a visible photon is absorbed by the dye, the excited-state dye is quenched by electron injection into the TiO_2 conduction band. The photooxidized dye is then regenerated by capture of an electron from the valence band of CuSCN, a process also referred to as hole injection. The two photoseparated charges then percolate separately through the two phases and, in the absence of recombination, reach the front and back contacts, respectively. Recombination consists of either: (a) reduction of the oxidized dye by an electron from TiO_2 before hole injection into CuSCN regenerates the dye or (b) recombination of an electron from the TiO_2 with a hole in the CuSCN.

In continuing our research into the combination TiO_2/dye/CuSCN, we have recently published a synthetic approach leading to easy fabrication of cells that reach 2% energy efficiency.[26] These cells show good currents and acceptable voltages when compared with other solid-state dye-sensitized cells[16,17] or to the related polymer/fullerene cells.[27,28] However, the fill factors are frequently ≤ 0.5, whereas >0.6 is required for a viable photovoltaic technology. We have recently shown that the poor fill factor in TiO_2/dye/CuSCN cells is caused in part by a recombination rate at V_{oc} that is ≥ 20 times faster than that observed in liquid junction cells using the I^-/I_3^- redox couple.[23]

It has recently been shown that it is possible to increase the V_{oc} in dye-sensitized liquid-junction cells by coating the porous oxide films with a very thin conformal overlayer of an insulator (e.g., SiO_2, Al_2O_3, $SrTiO_3$).[11,29,30] The technique has also been

* Author to whom correspondence should be addressed. E-mail: oregan@ecn.nl.

10.1021/jp0468049 CCC: $30.25
Published on Web 02/19/2005

applied to solid-state dye-sensitized cells using CuI as the hole conductor.[31−33] In several publications, insulator-coated TiO_2 films have given an increase in efficiency relative to that of control cells. However, to the best of our knowledge, it has not yet been possible to surpass the best efficiencies reached by cells without insulator layers in either the electrolyte or solid-state case. It is clear that a more detailed understanding of the function of the coating is required to optimize performance.

There are three ways a surface coating can cause an increase in the V_{oc} of a dye-sensitized cell. In case 1, the insulating nature of the coating material means that photoinjected electrons in the TiO_2 can only recombine with a positive charge in the electrolyte or hole conductor by tunneling through the insulator. This is the "tunnel barrier" effect. The barrier causes a decrease in the "per electron" recombination rate constant for a given electron population. If, at 1 sun illumination, the flux of injected electrons from the dye is unchanged, then the electron concentration at V_{oc} will be higher for the cell with the coating. A larger electron concentration in the TiO_2 means a more negative Fermi level and thus a larger V_{oc}. In case 2, the "surface dipole" effect, the surface coating changes the distribution of charge across the TiO_2/hole conductor interface relative to the uncoated case. If the coating results in more negative charge closer to the TiO_2 surface, and more positive charge closer to the CuSCN, then the resulting electric field will increase the band offset between the two materials. This will not directly cause a decrease in the recombination rate constant at V_{oc}, so there will be no change in the concentration of electrons in the TiO_2 at V_{oc}. The increased band offset is the source of the increase in V_{oc}. In case 3, the coating removes, or moves out of the gap, a significant fraction of the surface states at potentials near V_{oc} so that the total density of states at these potentials is reduced. This might directly reduce the recombination rate constant if recombination occurred through surface states. There are strong indications that recombination is not limited by surface-state density, but rather by transport; thus, we can expect no change in the recombination rate constant for this case as well.[34,35] The population of electrons in the TiO_2 film at V_{oc} will not change, but the same 1 sun V_{oc} population of electrons will fill states closer to TiO_2 conduction band, resulting in a larger Fermi level offset and thus larger V_{oc}.

To improve the understanding of how the mix of these three effects results in the observed increase in voltage and fill factor, we have fabricated more than 40 cells with varying TiO_2 sources and thicknesses and number of Al_2O_3 layers. For 20 of these cells, we have used transient photovoltage measurements to determine the recombination rate constants as well as the density of states distribution (DOS). In this paper we present an initial analysis of these results.

Methods

Transparent conductive SnO_2 glass, "LOF Tec 8", nominal resistance 8 Ω/□, was purchased from Pilkington. A thin solid film of TiO_2 (30−100 nm) was deposited on the SnO_2 by spray pyrolysis.[36] Following this, 3−5 μm mesoporous layers of TiO_2 were deposited by one of two methods. For films of Degussa P25, we used an approach based on that of Lindström et al.[37] further described in ref 26. For films of colloidal TiO_2, colloidal anatase particles of mean diameter 30 nm were fabricated by hydrolysis of titanium isopropoxide (Aldrich) using a modification of standard recipes.[2,38,39] In this case, the autoclaving temperature was 230 °C for 12 h. The particles were dried at 60 °C and resuspended in a mixture of 2-propanol and terpinol. The viscosity was modified by the addition of methylcellulose. The films were doctor bladed onto the substrates with the spray pyrolysis underlayer. All TiO_2 layers were heated for ∼1 h at 450 °C in air. Thin Al_2O_3 layers were deposited into the mesoporous TiO_2 films following ref 11. Briefly, a 0.15 M solution of aluminum tri-*tert*-butoxide (Aldrich) was made in dry 2-propanol. The solution was made in a glovebox, but all further steps were performed in air. Prior to immersion in the coating solution, the TiO_2 films were rinsed in distilled water and then dried at 60 °C for 30 min. After immersion, the solution plus films was placed in a closed vessel and held at 60 °C for 30 min. The coated TiO_2 films were removed from the coating solution and quickly and thoroughly rinsed in either water or 2-propanol. We found that, under some conditions, water rinse tends to leave traces of Al_2O_3 on the outer surface of the TiO_2 film as well as on the exposed SnO_2 and the back of the glass support. The Al_2O_3 coating solution was stored in closed vessels, and air exposure was minimized. We found that, in humid conditions, there is a reaction of air humidity with the coating solution, leading to thicker and inhomogeneous coatings that can block the pores in the TiO_2.

After Al_2O_3 coating, the films were heated again to 450 °C, allowed to cool to ∼100 °C in air, and then placed in the ethanolic dye solution. The dye, $RuL_2(SCN)_2$ where L = 4,4′-dicarboxy-2,2′-bipyridine, known as "N3", was purchased from Solaronix under the name Ruthenium 535. In this form, the dye is intended to have four protons as counterions. After dyeing overnight, the films were removed from the dye solution and then dried by pressing the TiO_2 side down on absorbent paper. Directly after drying, the samples were placed onto the 80 °C hotplate used for CuSCN deposition.

CuSCN was deposited from solution into the pores of the TiO_2 films with slight modifications of the previously described technique.[26] Briefly, CuSCN (Aldrich) was dissolved to saturation (∼2 g/L) in dipropylsulfide (Merck or ACROS). In most cases, the CuSCN solutions were doped with 1−10 mol % Cu(II)$(SCN)_2$ several days prior to use. Cu(II)$(SCN)_2$ was made by precipitation from water solution of LiSCN and $CuClO_4$ followed by filtration, water rinse, and drying in vacuum. Before deposition, the solutions were diluted 20% by additional dipropylsulfide. The doped and diluted solutions provided the highest and most reproducible efficiencies. The CuSCN solution was spread onto the TiO_2/dye film at 80 °C in air by using a special apparatus.[26] The resulting composite cells were treated under low vacuum (∼5×10^{-2} millibar) for 2 h and then stored under nitrogen for several days before measurement. An improvement in performance was noted during storage in nitrogen, presumably because of the continued slow outgassing of the solvent from the CuSCN layer.[26] Alternatively, after deposition, the cells were heated for an additional 10−15 min at 80 °C in air and then stored in flowing nitrogen at 60 °C for 1 h. This treatment also seemed to remove the last vestiges of solvent.

Electrical contact was made to the CuSCN using a cell holder that presses a one-cm^2 pad of fine graphite powder (Aldrich) onto the surface. Evaporated gold contacts were found to give identical results. Potentials reported herein refer to the TiO_2 contact; thus, negative potentials indicate more electron-rich TiO_2.

Photocurrent vs voltage measurements were made using illumination from a Steuernagel solar simulator that contains a metal−halogen arc lamp. Photocurrent and photovoltage transients were taken using a pump pulse generated by a ring of red LEDs controlled by a fast solid-state switch. Pulse times of 100 μs were used, with a rise and fall time of ≤2 μs. The pulse

was incident on the SnO_2 side of the cell. The pulse intensity was controlled to keep the ΔV due to the pulse below 10 mV. White bias light, incident on the SnO_2 side of the cell, was supplied by 10 W "Solarc" lamps (WelchAllyn) that are also of the metal−halogen type. The bias light was attenuated when needed by neutral-density filters. When the pulse intensity from the red diodes was insufficient to give voltage signals greater than 0.5 mV, a white flash lamp was used. The flash time was also 100 μs, with a fall half time of 20 μs. The time resolution of the potentiostat is 20 μs; thus, we could measure transient phenomena with time constants $\geq$40 μs. It is important to note that both the Steuernagel and Solarc light sources contain a UV component similar to that found in sunlight. The TiO_2/N3/CuSCN cells usually show much better performance under such illumination than under incandescent (tungsten halogen) lamps lacking UV.[25]

Analysis

It has been previously shown that the transient photovoltage measured at the external contacts is a good measure of the transient offset of the Fermi level in the TiO_2 phase of the i-het.[23] This is because the doped CuSCN used in these cells has an acceptor density at least 1000 times higher than the donor density in the TiO_2.[40] Thus, in the dark, the Fermi level in both materials will be equal to the work function of the CuSCN. Under bias and/or pulse illumination, the same number of electrons are added to the TiO_2 and holes to the CuSCN. In the CuSCN, the proportional change in the hole density will be small, and the Fermi level will move much less than that in the TiO_2. Thus, both the V_{oc} generated by the bias light and the ΔV created by the pulse measure shifts of the Fermi level in the TiO_2.

In the photovoltage transients, the decays are very close to single exponential (see Figure 3). We have fit a single exponential to the decay and extracted the pseudo-first-order recombination rate constant (k_{pfo}). We use "pseudo" here, as the rate constant is not independent of electron concentration. We have also used the transient voltage data to calculate the capacitance and density of trap states (DOS) at each V_{oc}. The capacitance of the TiO_2/CuSCN interface can be calculated as $C = \Delta Q/\Delta V$, where ΔV is the peak of the transient and ΔQ is the number of electrons injected by the pulse. We find ΔQ by integrating a photocurrent transient at $V = 0$, caused by an identical pulse. This will underestimate the actual injected charge by the fraction of electrons that are lost to recombination during transport. We estimate this error to be less than 30% in the worst cases. More importantly, the error will affect only the magnitude and not the shape of the calculated capacitance or DOS vs potential curves. (We note that this capacitance is a "chemical capacitance" i.e., it is controlled by the density of states at the Fermi level. This capacitance will thus have a dependence on the applied voltage not found in a classical capacitor of two metallic conductors separated by an insulator.)

As a check on this method of measuring the capacitance, we have compared the total charge (Q_{tot}) in the cell at V_{oc} found by integrating the capacitance with that found by "charge extraction". In this latter method, a 1 sun LED illumination source is turned off in $<$1 μs, while simultaneously, the cell is switched from open to short circuit. The resulting current, as the cell returns to $V = 0$ and $J = 0$, is integrated to give a direct measurement of the excess charge in the film at V_{oc}.[41] The number of electrons measured is always a *lower bound* for the total electron density, given that some electrons may recombine internally instead of traveling through the external circuit. The agreement between the integrated capacitance and the charge extraction Q_{tot} is good. The charge extraction Q_{tot} is always between 5 and 30% smaller than the integrated capacitance.

In these nanoparticulate cells, including the electrolyte and solid-state cases, the capacitance measures the amount of charge that can be stored in traps both in the bulk of the TiO_2 particles and at the interface between the TiO_2 and the electrolyte or p-conductor.[42−44] This is because in the nanoparticulate TiO_2 layers, there are far more electrons in traps than in the conduction band.[5] There will also be a parallel contribution to the capacitance from the interface between the SnO_2 substrate and the electrolyte/hole conductor. However, to first order this contribution will be independent of potential, and can be ignored in the potential range where the capacitance of the i-het is large and increasing exponentially. The measured capacitance will be proportional to the DOS at that V_{oc} as long as the number of electrons per particle is not large enough to create an electric field in the particle. This holds at all potentials examined in this study. To calculate the DOS (in electron states/cm^3 V), we have used DOS $= (6.24 \times 10^{18})[C/(d(1 - p))]$, where C is the capacitance/cm^2, d is the thickness of the TiO_2 film in cm, p is the porosity, and the conversion factor is the number of electrons per coulomb. This DOS includes both surface and bulk traps.

Results and Discussion

Figure 1a shows photocurrent vs potential characteristics (IVs) at 1 sun illumination for P25/TiO_2/dye/CuSCN cells with and without Al_2O_3 layers. The nanoporous TiO_2 layers consisted of $\sim$4 μm of pressed and sintered P25 particles. The effect of one Al_2O_3 layer was to increase the voltage from 550 to 690 mV, while the photocurrent decreased from 7.2 to 5.1 mA. The fill factor increased from 0.46 to 0.59, and the efficiency increased from 1.8 to 2.1%. The addition of a second Al_2O_3 layer caused a further increase in the voltage to 0.79 V; however, photocurrent decreased to 3.3 mA and the fill factor to 0.57, leading to an efficiency decrease to 1.5%. This set of IVs shows one of the largest effects of Al_2O_3 layers that we have measured. As will be seen below, the trend shown in Figure 1a is always reproduced, although the magnitudes of the effects vary substantially.

Figure 1b shows three 1 sun IVs for cells where the nanoporous TiO_2 layer consisted of $\sim$3 μm of sintered colloidal particles ($\sim$30 nm diameter). For this example, the effect of one Al_2O_3 layer is to increase the voltage from 0.61 to 0.67 V and to decrease the photocurrent from 5 to 4 mA/cm^2. The fill factor is increased from 0.45 to 0.56, and the efficiency increases from 1.4 to 1.5%. The addition of a second layer causes a further increase in the voltage to 0.71 V and an increase in the fill factor to 0.58; however, the decrease in the photocurrent to 3.4 mA results in a decrease in the efficiency to 1.4%.

We have found that the quantitative effect of the Al_2O_3 layer depends not only on the thickness of the layer but also on the type of TiO_2 used, the characteristics of the CuSCN solution, and other uncontrolled factors. Figure 2 shows a bar graph summary of the IV results of six separate comparisons of cells with varying Al_2O_3 layers. The bars give the average percent change in the IV characteristics for one and two Al_2O_3 layers relative to that for the cells without Al_2O_3. The error bars give the range of the percent change across the six comparisons. For example, the application of one Al_2O_3 layer caused an average increase in V_{oc} of 17%, with a range from 8 to 28%. This was accompanied by an average decrease in photocurrent of 14%. Thus, on average, the photovoltage increase is nearly negated by the photocurrent decrease. The biggest change was in fill

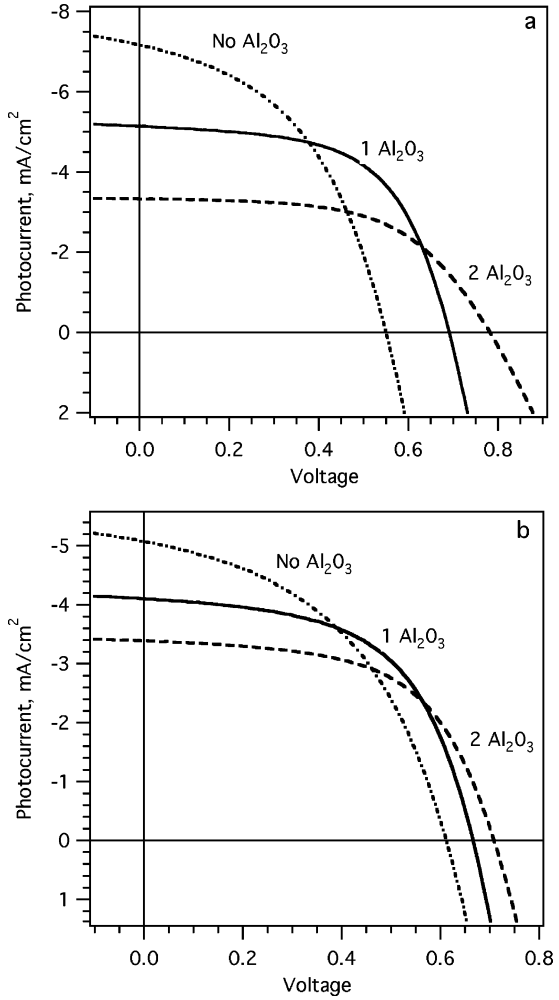

Figure 1. Photocurrent vs voltage results for TiO_2/(Al_2O_3)/dye/CuSCN cells with zero, one, and two Al_2O_3 layers. Illumination was 100 mW/cm^2 simulated AM1.5. Cell surface area was 1 cm^2. (a) TiO_2 layer of pressed P25 particles; thickness ~4 μm. (b) TiO_2 layer of 30 nm colloidal particles; thickness ~3 μm.

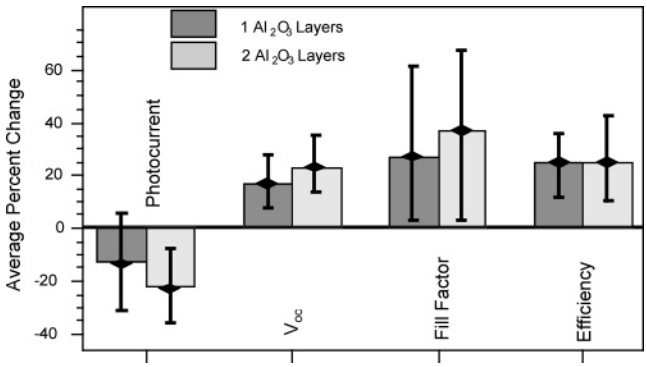

Figure 2. Summary of IV results from six comparisons of TiO_2/dye/CuSCN cells with zero, one, and two Al_2O_3 layers. The filled bars represent the average percentage change for the one- or two-Al_2O_3-layer cell, relative to the matched cell with no Al_2O_3. The "error" bars give the range of the results.

factor, where the average increase for one Al_2O_3 layer was 27%. The average increase in efficiency for one Al_2O_3 layer was 25%. For cells with two Al_2O_3 layers, the percent changes in photocurrent, voltage, and fill factor were all slightly larger, but the mean increase in efficiency was no better than for one Al_2O_3 layer.

Several important correlations are not apparent from the presentation in Figure 2. In general, the fractional increase in efficiency given by an Al_2O_3 layer was smaller when the comparison cell without Al_2O_3 had higher-than-average efficiency. Thus, the effect of the Al_2O_3 layers is not completely additive with respect to other methods of improving cell efficiency. For this reason, our record cell efficiencies are ~2.3% for cells with and without Al_2O_3 layers. More promisingly however, voltage increase and photocurrent decrease are not always linked. If the best measured voltage and FF increases that occurred without photocurrent loss could be added to the record cell without Al_2O_3, the efficiency should be around 3%.

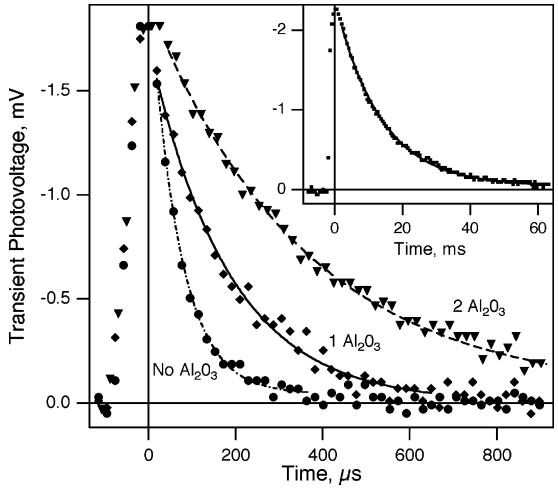

Figure 3. Normalized transient photovoltage curves at V_{oc} for TiO_2-(Al_2O_3)/dye/CuSCN cells with zero, one, and two Al_2O_3 layers. Bias illumination was ~100 mW/cm^2 white light giving V_{oc} of 570, 630, and 670 mV, respectively. Pulse from a white flash lamp, length 100 μs. Fit lines are single exponentials. (Inset) Transient photocurrent from cell with one Al_2O_3 layer under bias illumination ~0.1 mW/cm^2.

Unsurprisingly, the largest increases in fill factor came in comparison to base cells with the lowest fill factors. More interestingly, the largest increase in fill factor was also correlated with the largest decrease in photocurrent. Because of this, the largest increase in fill factor does not translate into an equivalent increase in efficiency. The largest increase in fill factor came from the thickest films (5 μm P25), consistent with the hypothesis that the low initial fill factor comes from the poor competition between transport and recombination in these cells. It is not clear why these cells should also show the largest decrease in photocurrent, but it could be related to lower success in pore filling with CuSCN because of the slightly smaller pore necks after Al_2O_3 addition.

As mentioned in the Introduction, there are several mechanisms by which the Al_2O_3 layer can cause an increase in V_{oc}. Photovoltage transients at V_{oc} can help elucidate which of these mechanisms is dominant. Figure 3 shows representative photovoltage transients for cells with zero, one, and two Al_2O_3 layers. The transients were taken at V_{oc} with 1 sun bias light. The signals have been normalized to the same height at time zero. The actual voltage peak of all transients was $\leq$3 mV. The lines through the data are fits to a single-exponential decay. The fits are quite good, as expected for the very small voltage perturbations. For TiO_2/dye/CuSCN layers, the decay of the voltage signal has been shown to depend on the rate of electron−hole recombination across the TiO_2/CuSCN interface. [23] From the exponential fits, we extract a pseudo-first-order rate constant (k_{pfo}) for the recombination reaction. The inverse of the rate constant is equivalent to the electron lifetime. From the data in Figure 3, the k_{pfo} for the cell with no Al_2O_3 is 1.3×10^4/s (lifetime 75 μs). Application of one Al_2O_3 layer decreases k_{pfo} to 5.5×10^3/s (lifetime 180 μs). The second Al_2O_3 layer causes

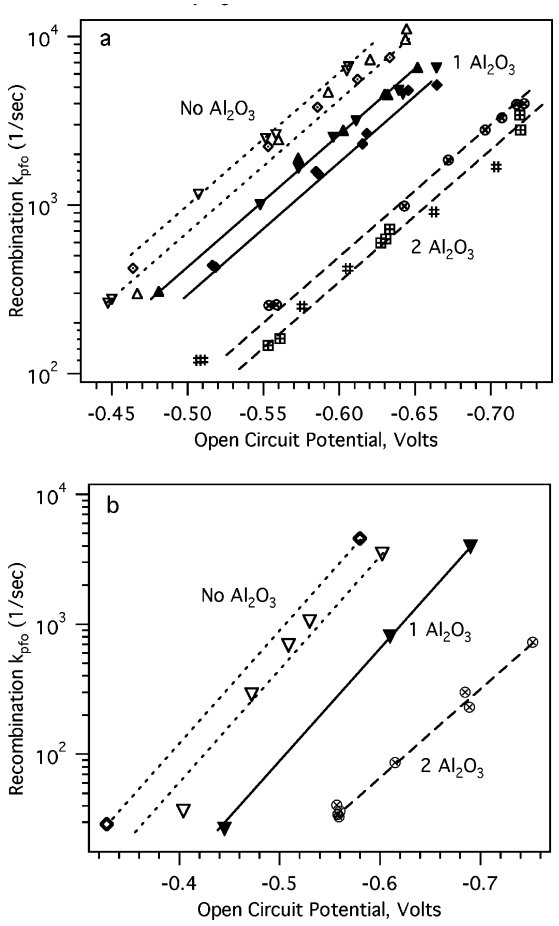

Figure 4. Pseudo-first-order recombination rate constant (k_{pfo}) vs V_{oc} for $TiO_2(Al_2O_3)$/dye/CuSCN cells with zero, one, and two Al_2O_3 layers. V_{oc} was varied by varying the bias light intensity. Flash intensities were varied to maintain a peak ΔV below 10 mV. (a) k_{pfo} vs V_{oc} for cells with colloidal TiO_2 layers. (b) k_{pfo} vs V_{oc} for cells with P25 TiO_2 layers.

another decrease to 2.7×10^3/s (lifetime 360 μs). Note that even with two Al_2O_3 layers, the electron lifetime is still more than 10 times shorter than that observed in TiO_2/dye/electrolyte cells, which is normally $\geq$5 ms at 1 sun V_{oc}.

The recombination rate constant can be measured as a function of potential by varying the bias light and thus the V_{oc}. The inset in Figure 3 shows an example of the photovoltage decay for a one-Al_2O_3-layer cell using bias illumination of 0.1 mW/cm^2. The pump pulse has been decreased to keep the voltage perturbation below 3 mV. The decay is still well fit by a single exponential. In this case, k_{pfo} has decreased to 76/s, giving a lifetime of 13 ms. The strong dependence of the recombination rate constant on V_{oc} is a key characteristic of both electrolyte and solid-state dye-sensitized cells.[45−48]

Figure 4a shows a log plot of k_{pfo} vs V_{oc} for nine cells with different numbers of Al_2O_3 layers. For this figure, all cells had $\sim$3 μm colloidal TiO_2 layers. The illumination level was varied from $\sim$0.1 to 100 mW/cm^2, and thereby, the V_{oc}, over a range of $\sim$240 mV. It is apparent that log(k_{pfo}) is linearly dependent on V_{oc}. A global fit to all data sets using a common slope gives a slope of 8.1 $\pm$ 0.2, corresponding to 120 mV/decade. The lines plotted in the figure are guides to the eye with this slope. The Al_2O_3 layers cause a decrease in k_{pfo} for all potentials but do not cause a change in the slope. We take this to indicate that the deposition of Al_2O_3 does not change the underlying recombination mechanism. Also, the effect of the coating on k_{pfo} varies, but there is no overlap between the data for zero, one, or two coatings.

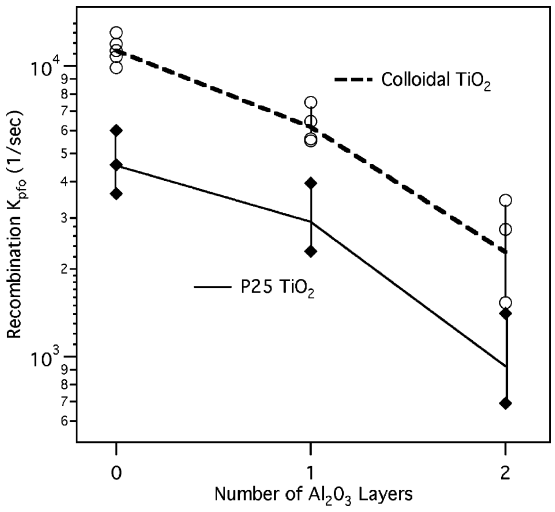

Figure 5. Recombination rate constant, k_{pfo}, at V_{oc} for $TiO_2(Al_2O_3)$/dye/CuSCN cells with either P25 or colloidal TiO_2 and zero, one, or two Al_2O_3 layers. Bias illumination was $\sim$100 mW/cm^2.

Figure 4b displays similar data for a less extensive data set with P25 TiO_2 layers. Here again, the decrease in k_{pfo} for one and two Al_2O_3 layers is obvious. The slope of the lines shown on this graph varies from 10% steeper than that shown by the colloidal TiO_2 cells, (for zero and one Al_2O_3 layer) to 13% flatter for two Al_2O_3 layers. Given these small deviations, it is reasonable to assume that the underlying recombination mechanism is the same for the two kinds of TiO_2.

Figure 5 shows the recombination rate constant k_{pfo} at 1 sun V_{oc} plotted vs the number of Al_2O_3 layers. Data are shown for 12 colloidal TiO_2 cells and 7 P25 cells. For the colloid cells, the average recombination rate constant without Al_2O_3 is 1.1 $\times$ 10^4/sec, decreasing to 6.2×10^3/s when one Al_2O_3 layer is present, and further to 2.3×10^3/s with two Al_2O_3 layers. The decreasing k_{pfo} at V_{oc} is already strong evidence that the tunnel barrier effect is providing some of the increase in V_{oc}. If only surface-dipole or surface-state passivation were occurring, then k_{pfo} at 1 sun V_{oc} would be expected to remain unchanged or possibly increase. For the P25 cells, almost the same trend is seen, except that the average recombination rate constants are $\sim$2.5 times slower than those for the colloidal TiO_2 cells.

The transient voltage data can also be used to calculate the capacitance and density of states (DOS) of the TiO_2 film at each V_{oc}. The capacitance is equal to the charge injected during the flash divided by the peak voltage of the transient. The capacitance can be converted directly to the density of trap states, taking into account the thickness and porosity of the TiO_2 films. Details are discussed in the Methods section. Figure 6a shows capacitance vs V_{oc} curves for five TiO_2/dye/CuSCN cells with P25 or colloidal TiO_2 and various Al_2O_3 layers. The right axis in Figure 6a shows the corresponding DOS scale appropriate for the 3 μm colloidal TiO_2 films. (The axis cannot hold simultaneously for the P25 data because of the different layer thickness.) We have fit the capacitance/DOS data to a single exponential using eq 1.

$$C(V) = K + C_o\, e^{(-V/m_c)} \qquad (1)$$

The value of m_c, the "characteristic energy", describes the curvature of the DOS distribution. The DOS vs V_{oc} curve is fit well by a single exponential, as has been found by other authors.[42,47,49] For the colloidal TiO_2/dye/CuSCN cells, m_c lies between 50 and 65 mV with uncertainties on the order of $\pm$15 mV at the 95% confidence level. Using the same transient

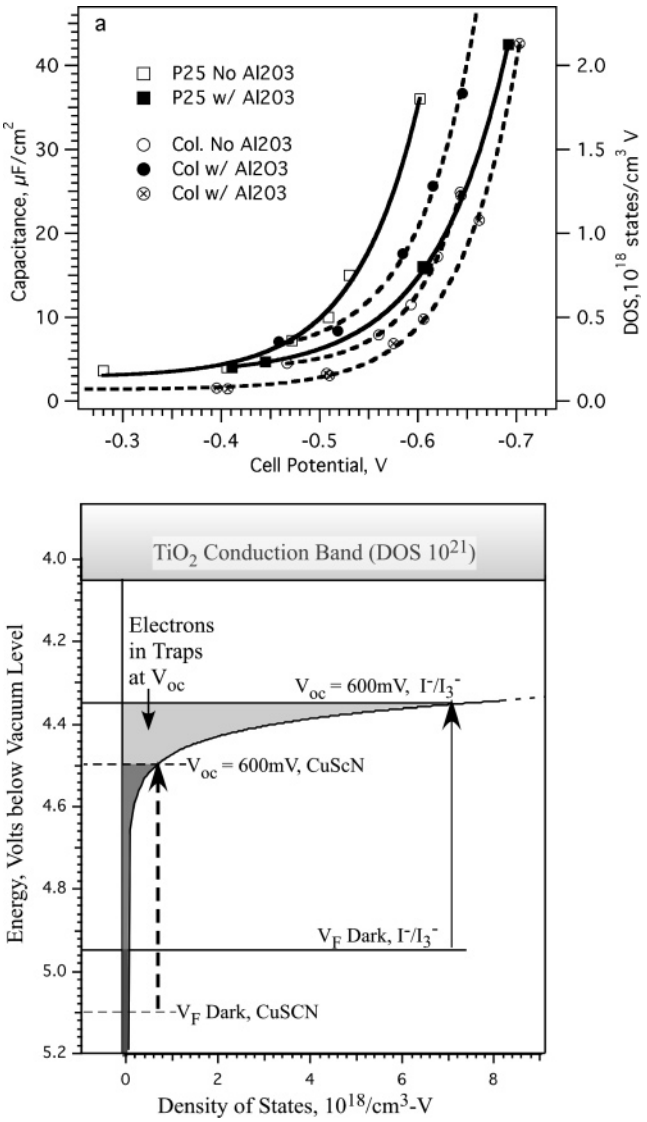

Figure 6. (a) Capacitance vs voltage for TiO_2/dye/CuSCN cells. (b) Density of states versus vacuum level diagram. Note that the bottom axis in part a is equivalent to the left axis in part b.

measurement for TiO_2/dye/electrolyte cells we find $m_c = 64-73$ mV. Similar m_c values have been reported for electrolyte cells measured by other methods such as EIS (69 mV)[47] or "charge extraction" (68 mV).[49] On the basis of these data, the DOS distribution measured via the transients is in agreement with that measured by other techniques. Also, the similar m_c for the solid-state and electrolyte cells is consistent with the assertion that the measured DOS is that of the TiO_2 in both cases.

In Figure 6b, a DOS distribution with an m_c of 65 mV is displayed with potential (relative to vacuum level) on the vertical scale and DOS on the horizontal. The DOS distribution curve does not extend up to the conduction band edge because of the scale of the bottom axis.[50] Also included is a reasonable level for the TiO_2 conduction band edge and the work functions of CuSCN and the I^-/I_3^- electrolyte.[23] To show the Fermi level in the TiO_2 at a given V_{oc}, we added the V_{oc} to the work function of the respective hole conductor. It is evident that the same V_{oc} in both types of cells results in Fermi levels in the TiO_2 that are at different depths below the conduction band edge, and therefore not at the same position in the DOS distribution. This explains the large difference in the DOS measured for the two kinds of cells. At $V_{oc} = 600$ mV, the measured DOS for the TiO_2/dye/CuSCN cells without Al_2O_3 averages $7.5 \times 10^{17}/cm^3$. At the same V_{oc} in a "standard" electrolyte cell (containing imidazolium iodide, LiI, and *tert*-butylpyridine), we measured a DOS of 4×10^{18}, or 5.3 times higher than for the CuSCN cells. In Figure 6b, we have assumed that the surface dipole at the TiO_2/(hole conductor) interface is identical in the two types of cells. This allowed us to set the difference between the TiO_2 Fermi levels at $V_{oc} = 600$ mV equal to the difference in work function of I^-/I_3^- and CuSCN. The data support this assumption in the following way. The observed 5.3-fold increase in DOS for the electrolyte cell, in combination with a DOS distribution with $m_c = 65$ mV, implies that the TiO_2 Fermi level is 110 mV closer to the conduction band in the electrolyte cell than in the CuSCN cell. This is in fair agreement with the 150 mV smaller work function for I^-/I_3^- relative to CuSCN.

In Figure 6a, it can be seen that there are shifts in the "onset potential" for the DOS distributions of the different cells. These shifts can be due to changes in the band offset between CuSCN and TiO_2. Alternately, the change in the DOS onset could be caused by chemical changes in the nature of the trap states caused by the application of the Al_2O_3 layer. It would seem likely that passivation of >50% of the surface states would result in some change in the shape of the DOS distribution. Because the shape of the DOS curve (m_c) is only very slightly modified by the Al_2O_3 application, it seems that chemical changes are less likely than surface dipole changes. Overall, from the 14 colloidal TiO_2 cells measured, we find that the DOS onset varies up to 40 mV for supposedly identical cells.[51]

The variation in "identical" cells makes it difficult to determine if the Al_2O_3 layer causes a shift in the DOS onset. The average shift for cells with one Al_2O_3 layer is ~15 mV and, thus, is buried beneath the intrinsic variation. Note that for the colloidal TiO_2 example shown in Figure 6a, the apparent shift in the capacitance onset for the one Al_2O_3 layer cell is +30 mV, where the same cell showed a shift in V_{oc} of −20 mV. Thus, in this particular case, the shift in band offset worked against the voltage increase caused by the reduction in the recombination rate constant.

For the cells with two Al_2O_3 layers, the negative shift in the capacitance onset is at most 50 mV, also barely above the variation of identical cells. Comparing the onset shift of each cell with the increase in V_{oc}, we conclude that surface dipole effects from Al_2O_3 explain less than 50% of the observed increase in the V_{oc}. For the smaller P25 TiO_2 data set, the three P25 cells with Al_2O_3 showed a negative shift in the capacitance curve relative to the three cells without Al_2O_3. However, the size of the shift did not correlate with the increase in the V_{oc}. In sum, the presence of a clear change in k_{pfo}, and an upper limit on the effects of band offset, shows that the tunnel barrier effect is the most significant contributor to the increase in V_{oc}.

We now consider the effect of the Al_2O_3 layers on the fill factor. We have recently presented a model that explains the low fill factors in TiO_2/dye/CuSCN cells based on the relationship of recombination rate and electron mobility in the TiO_2 as a function of the Fermi level.[23] We refer the reader to ref 23 for the details of the argument. The model predicts that a V_{oc} increase caused by a decrease in the recombination rate constant should be accompanied by an increase in the fill factor, whereas increasing the band offset between TiO_2 and CuSCN will not increase the fill factor. The increases in fill factor seen in the data, along with the lack of obvious band edge shift, are consistent with this model. Going further, there is one matched pair of one Al_2O_3 layer cells with a 45 mV difference in the

position of the capacitance onset. Consistent with the model, the cell that showed a capacitance onset at the lower voltage, meaning the smallest contribution of band offset, showed a significantly higher fill factor, 56% compared to 47%. This one comparison is clearly not proof, but it does indicate the power of combined capacitance, recombination, and IV measurements to construct and test models of the cell's operation.

We can use the recombination rate constant and capacitance data to examine the internal consistency of the conclusions reached in the previous paragraphs. We note that, at V_{oc}, eq 2 relates the injection and recombination current to k_{pfo} and Q_{tot}, where Q_{tot} is the number of electrons added to the TiO_2 film between $V = 0$ and V_{oc}.

$$J_{rec} = J_{inj} = \alpha Q_{tot} k_{pfo} \quad (2)$$

By definition, at V_{oc} the recombination current (J_{rec}) is equal to the injection current (J_{inj}). Under the assumption that all electrons are indistinguishable over the time scale of the recombination, α is equal to one. This assumption is not always valid for dye-sensitized TiO_2 cells.[52] The value of α does not affect the following consistency check. We discuss the actual value of α further below.

We make the assumption that the decrease in photocurrent for the one-layer Al_2O_3 cells (average ~20%) results from decreased injection. From eq 2, we calculate the increase in the Q_{tot} implied by the change in J_{inj} and k_{pfo} between zero and one Al_2O_3 layer. The observed factor 2 decreases in k_{pfo} (Figure 5) gives an increase in Q_{tot} by a factor of 1.6. Following the capacitance vs voltage curve with $m_c = 65$ mV, a factor of 1.6 increase in Q_{rec} implies a 30 mV increase in V_{oc}. This is most of the ~40 mV average shift seen in the samples used for transient studies.

This approach can also be used to rationalize why the lower recombination rate constants seen for the P25 films (Figure 5) did not result in a higher V_{oc}. We measured three P25 cells with no Al_2O_3. These films showed ~3 times higher capacitance for a given voltage than the colloidal TiO_2 films. Because the P25 films are 33% thicker, the capacitance normalized to the same thickness will be 2.3 times higher. At a given V_{oc} the number of electrons (Q_{tot}) in the P25 film will be 2.3 times higher. From formula 2, we see that the 2.5-fold decrease in k_{pfo} will be canceled by the 2.3-fold increase in Q_{tot} so that the recombination current for a given V_{oc} hardly changes. For a given injection current, the V_{oc} for the P25 and colloidal films will be similar. More significantly this observation is consistent with the hypothesis that the recombination rate is limited by transport, which is in turn limited by trap density.[34,35,53]

The fact that the second Al_2O_3 layer always causes a decrease in efficiency indicates that the present deposition technique gives layers that are too thick. This implies the need for a thinner layer at each deposition step, which might be accomplished by drying the TiO_2 at a higher temperature before immersion in the deposition solution. It has been hypothesized that the deposition of the Al_2O_3 layer depends on the water absorbed at the TiO_2 surface after the 60 °C drying.[11] If so, this might explain some of the thickness variation, as the amount of adsorbed water may depend on the drying time and the ambient humidity. More careful drying of the TiO_2 will only work if water in the Al_2O_3 solution plays no role in the deposition, which is not yet known. Deposition of 1 nm of Al_2O_3 on 10 cm^2 of 3-μm thick colloidal TiO_2 requires only 0.7 mg of water. A typical cell holder will use at least 15 mL for the deposition. For the water on the TiO_2 to be limiting, 15 mL of solution should have less than 1 mg water, equivalent to <0.005 wt %. No source of 2-propanol is this dry, and in any case, a few minutes exposure to humid air could suffice to supply more than this amount of water. The preheating step mentioned in ref 11 may help reduce the water content of the deposition solution before insertion of the TiO_2 film. It is important to determine the role, if any, of air humidity on the deposition before further optimization can occur.

We now return to the fact that α in eq 2 is significantly smaller than one for dye-sensitized TiO_2 cells. For example, for one cell without Al_2O_3, integrating the capacitance from $V = 0$ to V_{oc} gives 2 $\mu C/cm^2$ for Q_{tot}, and the charge-extraction method gives a lower bound of 1.7 $\mu C/cm^2$. For this cell, the recombination rate constant at V_{oc} was 1.4×10^4. Applying eq 2 with $\alpha = 1$ gives an estimated recombination current of 28 mA/cm^2, with a lower bound of 24 mA/cm^2 using the Q_{tot} from charge extraction. These estimates are clearly too large. For this cell, the 1 sun plateau photocurrent was 5.7 mA/cm^2. The injection current cannot have been higher than 7 mA/cm^2, given the dye used and the TiO_2 film thickness of ~2 μm. For another cell with two layers of Al_2O_3, the integrated capacitance gives $Q_{tot} = 2.9$ $\mu C/cm^2$, and the recombination rate constant is 1×10^4. The estimated recombination current is thus 29 mA/cm^2, again clearly much too high for a 2-μm TiO_2 film. Although the value of Q_{tot} found by integrating the capacitance can have several sources of error, the value of Q_{tot} from charge extraction is a secure lower bound, thus an $\alpha < 1$ is required. In general, values of α between 0.2 and 0.3 give recombination currents no higher than the maximum possible injection currents. We have also measured seven dye-sensitized electrolyte cells that also gave $\alpha = 0.2-0.35$.

A full discussion of α is not within the scope of this paper. Values of $\alpha < 1$ might arise from transport-limited recombination and/or by trapping/detrapping times that are longer than the recombination time scale. An analogous discrepancy has been observed when comparing the measured Q_{tot} at short circuit and the Q_{tot} calculated from the short-circuit photocurrent and the photocurrent characteristic time.[52]

Conclusions

From our analysis, the Al_2O_3 layer does produce the intended tunnel barrier effect. The similar trends of rate constant with V_{oc} indicate that the aluminum oxide does not cause a significant change in the recombination mechanism. The similar curvatures and positions of the DOS curves indicate there is little change in the band edge potential and the curvatures and positions are consistent with little change in the existence or occupation of surface states. It should be possible to construct Al_2O_3-coated cells that surpass the record efficiencies of uncoated cells. To achieve this, control of the coating thickness will need to be improved to avoid photocurrent losses from reduced injection and to avoid blocked pores. However, as the unexpected value of α in eq 2 makes clear, it is important to achieve a better understanding of the mechanism of recombination. If there are indeed widely spaced recombination "hot spots", then treatments aimed directly at these spots may be more rewarding than coating all of the particles with tunnel barriers.

References and Notes

(1) Desilvestro, J.; Gratzel, M.; Kavan, L.; Moser, J.; Augustynski, J. *J. Am. Chem. Soc.* **1985**, *107*, 2988.

(2) O'Regan, B.; Grätzel, M. *Nature* **1991**, *353*, 737.

(3) Nazeeruddin, M. K.; Péchy, P.; Renouard, T.; Zakeeruddin, S. M.; Humphry-Baker, R.; Comte, P.; Liska, P.; Cevey, L.; Costa, E.; Shklover, V.; Spiccia, L.; Deacon, G. B.; Bignozzi, C. A.; Grätzel, M. *J. Am. Chem. Soc.* **2001**, *123*, 1613.

(4) Hinsch, A.; Kroon, J. M.; Kern, R.; Uhlendorf, I.; Holzbock, J.; Meyer, A.; Ferber, J. *Prog. Photovoltaics* **2001**, *9*, 425.
(5) van de Lagemaat, J.; Frank, A. J. *J. Phys. Chem. B* **2000**, *104*, 4292.
(6) Kuciauskas, D.; Freund, M. S.; Gray, H. B.; Winkler, J. R.; Lewis, N. S. *J. Phys. Chem. B* **2001**, *105*, 392.
(7) Gillaizeau-Gautheir, I.; Odobel, F.; Alebbi, M.; Argazzi, R.; Costa, E.; Bignozzi, C. A.; Qu, P.; Meyer, G. J. *Inorg. Chem.* **2001**, *40*, 6073.
(8) Gregg, B. A.; Pichot, F.; Ferrere, S.; Fields, C. L. *J. Phys. Chem. B.* **2001**, *105*, 1422.
(9) Nakade, S.; Matsuda, M.; Kambe, S.; Saito, Y.; Kitamura, T.; Sakata, T.; Wada, Y.; Mori, H.; Yanagida, S. *J. Phys. Chem. B* **2002**, *106*, 10004.
(10) Yoshida, T.; Oekermann, T.; Okabe, K.; Schlettwein, D.; Funabiki, K.; Minoura, H. *Electrochemistry* **2002**, *70*, 470.
(11) Palomares, E.; Clifford, J.; Haque, S. A.; Lutz, T.; Durrant, J. R. *J. Am. Chem. Soc.* **2003**, *125*, 475.
(12) Chappel, S.; Chen, S. G.; Zaban, A. *Langmuir* **2002**, *18*, 3336.
(13) Yamamoto, J.; Tan, A.; Shiratsuchi, R.; Hayase, S.; Chenthamarakshan, C. R.; Rajeshwar, K. *Adv. Mater. (Weinheim, Ger.)* **2003**, *15*, 1823.
(14) Tennakone, K.; Senadeera, G. K. R.; De Silva, D. B. R. A.; Kottegoda, I. R. M. *Appl. Phys. Lett.* **2000**, *77*, 2367.
(15) Konno, A.; Kumara, G. R. A.; Hata, R.; Tennakone, K. *Electrochemistry* **2002**, *70*, 432.
(16) Krüger, J.; Plass, R.; Cevey, L.; Piccirelli, M.; Grätzel, M.; Bach, U. *Appl. Phys. Lett.* **2001**, *79*, 2085.
(17) Kumara, G. R. A.; Konno, A.; Shiratsuchi, K.; Tsukahara, J.; Tennakone, K. *Chem. Mater.* **2002**, *14*, 954.
(18) Krüger, J.; Plass, R.; Grätzel, M.; Cameron, P. J.; Peter, L. M. *J. Phys. Chem. B* **2003**, *107*, 7536.
(19) O'Regan, B.; Schwartz, D. T. *Chem. Mater.* **1995**, *7*, 1349.
(20) O'Regan, B.; Schwartz, D. T. Efficient Photo-Hole Injection from Cyanine Dyes into CuSCN: A Prospective p-Type Material for a Dye-Sensitized p−n Heterojunction. In *Nanostructured Materials in Electrochemistry*; Electrochemical Society: Reno, NV, 1995.
(21) Kumara, G. R. R. A.; Konno, A.; Senadeera, G. K. R.; Jayaweera, P. V. V.; De Silva, D. B. R. A.; Tennakone, K. *Sol. Energy Mater. Sol. Cells* **2001**, *69*, 195.
(22) Tennakone, K.; Kahanda, M.; Kasige, C.; Abeysooriya, P.; Wijayanayaka, R. H.; Kaviratna, P. *J. Electrochem. Soc.* **1984**, *131*, 1574.
(23) O'Regan, B. C.; Lenzmann, F. *J. Phys. Chem. B* **2004**, *108*, 4342.
(24) Perera, V. P. S.; Pitigala, P. K. D.; Jayaweera, P. V. V.; Bandaranayake, P. K. M.; Tennakone, K. *J. Phys. Chem. B* **2003**, *107*, 13758.
(25) O'Regan, B.; Schwartz, D. T. *Chem. Mater.* **1998**, *10*, 1501.
(26) O'Regan, B.; Lenzmann, F.; Muis, R.; Wienke, J. *Chem. Mater.* **2002**, *14*, 5023.
(27) Shaheen, S. E.; Brabec, C. J.; Sariciftci, N. S.; Padinger, F.; Fromherz, T.; Hummelen, J. C. *Appl. Phys. Lett.* **2001**, *78*, 841.
(28) Kroon, J. M.; Wienk, M. M.; Verhees, W. J. H.; Hummelen, J. C. *Thin Solid Films* **2002**, *403*, 223.
(29) Kumara, G. R. R. A.; Tennakone, K.; Prera, V. P. S.; Konno, A.; Kaneko, S.; Okuya, M. *J. Phys. D: Appl. Phys.* **2001**, *34*, 868.
(30) Kay, A.; Gratzel, M. *Chem. Mater.* **2002**, *14*, 2930.
(31) Taguchi, T.; Zhang, X.-T.; Sutanto, I.; Tokuhiro, K.; Rao, T. N.; Watanabe, H.; Nakamori, T.; Uragami, M.; Fujishima, A. *Chem. Commun.* **2003**, 2480.
(32) Zhang, X.-T.; Liu, H.-W.; Taguchi, T.; Meng, Q.-B.; Sato, O.; Fujishima, A. *Sol. Energy Mater. Sol. Cells* **2004**, *81*, 197.
(33) Tennakone, K.; Bandara, J.; Bandaranayake, P. K. M.; Kumara, G. R. A.; Konno, A. *Jpn. J. of Appl. Phys., Part 2* **2001**, *40*, L732.
(34) Nelson, J.; Haque, S. A.; Klug, D. R.; Durrant, J. R. *Phys. Rev. B: Condens. Matter Mater. Phys.* **2001**, *6320*, 5321.
(35) Kopidakis, N.; Benkstein, K. D.; van de Lagemaat, J.; Frank, A. J. *J. Phys. Chem. B* **2003**, *107*, 11307.
(36) O'Regan, B.; Schwartz, D. T. *J. Appl. Phys.* **1996**, *80*, 4749.
(37) Lindström, H.; Magnusson, E.; Holmberg, A.; Södergren, S.; Lindquist, S. E.; Hagfeldt, A. *Sol. Energy Mater. Sol. Cells* **2002**, *73*, 91.
(38) Anderson, M. A.; Gieselmann, M. J.; Xu, Q. *J. Membr. Sci.* **1988**, *39*, 243.
(39) Thomas, I. M. *Applied Opt.* **1987**, *26*, 4688.
(40) The evidence for the higher acceptor density is as follows. The dark conductivity of the CuSCN is $>10^4$ times larger than that of the TiO_2 film. Although the hole mobility of CuSCN is not known, it is likely to be similar to or smaller than that of CuI ($\sim$10 cm^2/V s) and thus no larger than the electron mobility of anatase TiO_2. Making the conservative assumption that the hole and electron mobilities are the same, the $>10^4$ times larger conductivity in CuSCN means that there are $>10^4$ times more holes in the CuSCN valence band than electrons in the TiO_2 conduction band. This estimate ignores several factors that might decrease (or increase) this ratio; however, they would not change the conclusion that CuSCN has the higher concentration of carriers.
(41) Duffy, N. W.; Peter, L. M.; Rajapakse, R. M. G.; Wijayantha, K. G. U. *J. Phys. Chem. B* **2000**, *104*, 8916.
(42) Willis, R. L.; Olson, C.; O'Regan, B.; Lutz, T.; Nelson, J.; Durrant, J. R. *J. Phys. Chem. B* **2002**, *106*, 7605.
(43) Peter, L. M.; Duffy, N. W.; Wang, R. L.; Wijayantha, K. G. U. *J. Electroanal. Chem.* **2002**, *524*, 127.
(44) Fabregat-Santiago, F.; Garcia-Belmonte, G.; Bisquert, J.; Zaban, A.; Salvador, P. *J. Phys. Chem. B* **2002**, *106*, 334.
(45) Huang, S. Y.; Schlichthorl, G.; Nozik, A. J.; Gratzel, M.; Frank, A. J. *J. Phys. Chem. B* **1997**, *101*, 2576.
(46) Liu, Y.; Hagfeldt, A.; Xiao, X. R.; Lindquist, S. E. *Sol. Energy Mater. Sol. Cells* **1998**, *55*, 267.
(47) van de Lagemaat, J.; Park, N.-G.; Frank, A. J. *J. Phys. Chem. B* **2000**, *104*, 2044.
(48) Fisher, A. C.; Peter, L. M.; Ponomarev, E. A.; Walker, A. B.; Wijayantha, K. G. U. *J. Phys. Chem. B* **2000**, *104*, 949.
(49) Duffy, N. W.; Peter, L. M.; Rajapakse, R. M. G.; Wijayantha, K. G. U. *Electrochem. Commun.* **2000**, *273*.
(50) Extending the measured DOS distribution to the assumed conduction band edge, $\sim$1 V above the CuSCN potential, gives an integrated density of traps of $5 \times 10^{19}/cm^3$ or one trap for about every 1000 Ti atoms. For 20-nm particles, this is equivalent to $\sim$200 traps/particle, which is consistent with measurements and model results. See ref 34 and Ikeda, S.; Sugiyama, N.; Murakami, S.; Kominami, H.; Kera, Y.; Noguchi, H.; Uosaki, K.; Torimoto, T.; Ohtani, B. *Phys. Chem. Chem. Phys.* **2003**, *5*, 778.
(51) A possible cause of this variation is different amounts of water and/or protons at the TiO_2 interface. This could be caused by slight differences in the dye solutions and by differences in the drying time before and after CuSCN application.
(52) van de Lagemaat, J.; Kopidakis, N.; Neale, N. R.; Frank, A. J. *Phys. Rev. B: Condens. Matter Mater. Phys.* **2004**. Accepted for publication.
(53) Nelson, J.; Chandler, R. E. *Coord. Chem. Rev.* **2004**, *248*, 1181.